

University of Kentucky

UKnowledge

Theses and Dissertations--Biomedical
Engineering

Biomedical Engineering


2021

CHARACTERIZATION OF MODULATION AND COHERENCE IN SENSORIMOTOR RHYTHMS USING DIFFERENT ELECTROENCEPHALOGRAPHIC SIGNAL DERIVATIONS

Stephen Dundon

University of Kentucky, srdundon@gmail.com

Author ORCID Identifier:

 <https://orcid.org/0000-0001-5486-4507>

Digital Object Identifier: <https://doi.org/10.13023/etd.2021.224>

[Right click to open a feedback form in a new tab to let us know how this document benefits you.](#)

Recommended Citation

Dundon, Stephen, "CHARACTERIZATION OF MODULATION AND COHERENCE IN SENSORIMOTOR RHYTHMS USING DIFFERENT ELECTROENCEPHALOGRAPHIC SIGNAL DERIVATIONS" (2021). *Theses and Dissertations--Biomedical Engineering*. 70.

https://uknowledge.uky.edu/cbme_etds/70

This Master's Thesis is brought to you for free and open access by the Biomedical Engineering at UKnowledge. It has been accepted for inclusion in Theses and Dissertations--Biomedical Engineering by an authorized administrator of UKnowledge. For more information, please contact UKnowledge@lsv.uky.edu.

STUDENT AGREEMENT:

I represent that my thesis or dissertation and abstract are my original work. Proper attribution has been given to all outside sources. I understand that I am solely responsible for obtaining any needed copyright permissions. I have obtained needed written permission statement(s) from the owner(s) of each third-party copyrighted matter to be included in my work, allowing electronic distribution (if such use is not permitted by the fair use doctrine) which will be submitted to UKnowledge as Additional File.

I hereby grant to The University of Kentucky and its agents the irrevocable, non-exclusive, and royalty-free license to archive and make accessible my work in whole or in part in all forms of media, now or hereafter known. I agree that the document mentioned above may be made available immediately for worldwide access unless an embargo applies.

I retain all other ownership rights to the copyright of my work. I also retain the right to use in future works (such as articles or books) all or part of my work. I understand that I am free to register the copyright to my work.

REVIEW, APPROVAL AND ACCEPTANCE

The document mentioned above has been reviewed and accepted by the student's advisor, on behalf of the advisory committee, and by the Director of Graduate Studies (DGS), on behalf of the program; we verify that this is the final, approved version of the student's thesis including all changes required by the advisory committee. The undersigned agree to abide by the statements above.

Stephen Dundon, Student

Dr. Sridhar Sunderam, Major Professor

Dr. Sridhar Sunderam, Director of Graduate Studies

CHARACTERIZATION OF MODULATION AND COHERENCE IN
SENSORIMOTOR RHYTHMS USING DIFFERENT
ELECTROENCEPHALOGRAPHIC SIGNAL DERIVATIONS

THESIS

A thesis submitted in partial fulfillment of the requirements for the degree of
Master of Science in Biomedical Engineering
in the College of Engineering at the University of Kentucky

By

Stephen Roy Dundon

Lexington, Kentucky

Director: Dr. Sridhar Sunderam, Professor of Biomedical Engineering

Lexington, Kentucky

2021

Copyright © Stephen Roy Dundon 2021
<https://orcid.org/0000-0001-5486-4507>

ABSTRACT OF THESIS

CHARACTERIZATION OF MODULATION AND COHERENCE IN SENSORIMOTOR RHYTHMS USING DIFFERENT ELECTROENCEPHALOGRAPHIC SIGNAL DERIVATIONS

Electroencephalography (EEG) is a widely used technique for monitoring and analyzing brain activity in experimental, diagnostic, and therapeutic applications. Since EEG is sensitive to noise and artefact sources, referential signals at different locations can be combined in different ways to improve signal quality and better localize cortical activity. Four signal derivations were compared against referential EEG in terms of their ability to measure the alpha rhythm modulation (or reactivity) and spatial coherence associated with an eye closure task: a common average reference (CAR), a local average reference (LAR), a large Laplacian (LL), and a focal Laplacian (FL) estimated using a specialized electrode. Results showed significant differences in the alpha reactivity averaged across all electrodes between EEG derivations: the CAR showed significantly greater reactivity than all other derivations while the LL showed significantly lower reactivity compared to all other derivations. No significant differences in alpha reactivity were found between the referential EEG, LAR, and FL when averaged across all locations. LL and FL displayed a trend of increasing alpha reactivity from frontal to occipital regions while the CAR and LAR showed no such trend. The referential EEG showed a linear decrease in spatial coherence as distance increased while the FL showed an exponential decrease. Further, the referential EEG showed no change in spatial coherence related to eye closure while all other derivations showed a significant increase. The focal Laplacian improves detection of alpha reactivity and signal localization without the need for multiple electrodes.

KEYWORDS: EEG, Tripolar EEG, Hilbert Transform, Spatial Filter, Mean Phase Coherence

Stephen Roy Dundon

(Name of Student)

6/16/2021

Date

CHARACTERIZATION OF MODULATION AND COHERENCE IN
SENSORIMOTOR RHYTHMS USING DIFFERENT
ELECTROENCEPHALOGRAPHIC SIGNAL DERIVATIONS

By
Stephen Roy Dundon

Dr. Sridhar Sunderam

Director of Thesis

Dr. Sridhar Sunderam

Director of Graduate Studies

6/16/2021

Date

ACKNOWLEDGMENTS

Though the following thesis is an individual work it benefited from, and likely would not exist without, the insights, direction, and support from several people. First, my advisor, Dr. Sridhar Sunderam, for offering me the opportunity to do this research and his tireless efforts to help me clarify my work. His dedication to his scholarship and students is an inspiration. In addition, I would like to thank Dr. Amir al-Bakri and Chase Haddix, for their support and instruction when I was first starting out in EEG research. Finally, in addition to the technical assistance of those above I would like to thank my family and friends for believing in me even when I didn't.

TABLE OF CONTENTS

ACKNOWLEDGMENTS	iii
LIST OF TABLES	vi
CHAPTER 1. Introduction	1
1.1 Motivation	1
1.2 Overview of Approach.....	2
1.3 Background	2
1.3.1 EEG and Neurophysiology	2
1.3.2 Alpha Waves.....	3
CHAPTER 2. Methods.....	4
2.1 Overview.....	4
2.2 Data Collection	4
2.2.1 Subjects.....	4
2.2.2 Tripolar Concentric Ring Electrodes	4
2.2.3 Tasks.....	5
2.3 Signal Analysis	7
2.3.1 Overview.....	8
2.3.2 Common Average Reference.....	8
2.3.3 Local Average Reference.....	9
2.3.4 Laplacian.....	9
2.3.5 Electrode Holders	14
2.4 Amplitude of event-related alpha modulation in terms of signal power.....	17
2.5 Spatial localization measured through signal coherence.....	18
CHAPTER 3. Results	20
3.1 Effect of Impedance on Powerline Noise and Alpha Detection.....	20
3.2 Effect of Spatial Filtering on the Strength of Alpha Reactivity	22
3.3 Effect of Spatial Filtering on Alpha Band EEG Coherence Between Regions	25
CHAPTER 4. Discussion.....	29
4.1 Overview.....	29
4.2 Impedance vs Preparation Time.....	29
4.3 Alpha Reactivity to Eye closure.....	29
4.4 Relation between MPC and Electrode Placement.....	31
4.5 Conclusion.....	32
4.6 Future directions	32

Bibliography	33
VITA.....	35

LIST OF TABLES

Table 1 Summary of statistics for the signal-impedance comparisons.....	22
---	----

LIST OF FIGURES

Figure 2.1 Subject seated with cap and electrodes on.	7
Figure 2.2 Close up of electrodes in the cap.....	7
Figure 2.3 Formula for calculating the voltage for a given location using the CAR method.	9
Figure 2.4 LAR formula for the F3 electrode.....	9
Figure 2.5 The Taylor series expansion for calculating the Laplacian for a location on a 2 dimensional grid.....	10
Figure 2.6 Example of a center electrode	11
Figure 2.7 Simplified formula for the Laplacian of a center electrode.....	11
Figure 2.8 Example of an edge electrode.....	12
Figure 2.9 Simplified formula for the Laplacian for an edge electrode.....	12
Figure 2.10 Example of a corner electrode.....	13
Figure 2.11 Simplified formula for the Laplacian of a corner electrode	13
Figure 2.12- EEG signal derivations.....	14
Figure 2.13 Electrode holder assembly.....	15
Figure 2.14 Electrode holder model seen from below.....	16
Figure 2.15 A TCRE in the holder.....	16
Figure 2.16 Formula for the calculation of mean phase coherence.	18
Figure 2.17 Proportional distances between electrodes in the montage.	19
Figure 3.1 Relation between the powerline noise in the signal and impedance	21
Figure 3.2 Relation between the alpha power in the signal and impedance	21
Figure 3.3 The average change in the magnitude of the Hilbert envelope of the alpha band in response to eye closure.	23

Figure 3.4 The distribution of the alpha reactivity of each region.....	24
Figure 3.5 The mean difference between the alpha reactivity of compared regions.	24
Figure 3.6 Mean phase coherence reactivity.....	26
Figure 3.7 MPC responses divided by the mean of the first 3 seconds	26
Figure 3.8 MPC vs Distance between electrodes for each of the signal derivations.	27
Figure 3.9 An illistative example of the MPC compared to distance	28
Figure 4.1 When the common average has significantly greater power.....	30

CHAPTER 1. INTRODUCTION

1.1 Motivation

Epilepsy is a seizure disorder that affects nearly 1% of the world's population (Mormann, Lehnertz, David, & Elger, 2000). Commonly held theories of the underlying pathology include abnormal neuronal synchronization that drives seizure propagation across the brain (Bragin, Engel Jr, Wilson, Fried, & Mathern, 1999). Electroencephalography (EEG) is a common tool for the diagnosis of various forms of epilepsy (Bartolomei et al., 1999). When seizures cannot be controlled through medication, areas of the brain believed to be epileptogenic zones may be surgically removed if they do not interfere with normal functions like speech and movement. Identification of these zones is done through analysis of intracranial EEG (iEEG) using electrodes placed directly on the cortex or inserted into deeper structures (Mormann et al., 2000; Schevon et al., 2007). Since placing an iEEG is an invasive procedure it is desirable to place the electrodes in as few locations as is necessary. A first approximate location may be determined through surface EEG and an improved localization of activity from the scalp is of great value.

EEG is usually obtained by measuring the electrical potential between each individual sensing electrode and a reference electrode affixed to a different location on the scalp with conductive gel; this is termed referential EEG measurement (Teplan, 2002). However, signal quality is critically dependent on preparing the scalp in a way that lowers the impedance between the sensing electrode and the reference as much as possible (Li, Wang, & Duan, 2017). Furthermore, since EEG is susceptible to many noise and artefact

sources, multiple referential signals are often combined in different ways to improve the signal-to-noise ratio and better localize cortical activity.].

1.2 Overview of Approach

This work is an attempt to determine how best to quantify and localize sensorimotor rhythm dynamics from the EEG. We compare four spatial filtering methods that combine multiple referential EEG (eEEG) signals against eEEG alone in terms of their ability to measure “alpha reactivity” – that is, the emergence of 8-13 Hz alpha oscillations in the EEG upon eye closure – in terms of their power and spatial synchrony measured using: 1. A common average reference (CAR); 2. A local average reference (LAR); 3. A large Laplacian approximation (LL), and a focal Laplacian (FL) estimated using a tripolar concentric ring electrode (TCRE). Further, a custom designed electrode cap was developed to make subject preparation faster and more convenient. The design is evaluated based on the quality of the signals in terms of electrode impedance and signal-to-noise ratio estimates gathered during this study.

1.3 Background

1.3.1 EEG and Neurophysiology

Electroencephalography (EEG) is a widely used technique for monitoring and analyzing brain activity in experimental, diagnostic, and therapeutic applications (Collinger et al., 2013; Guger et al., 2017; Luu, Nakagome, He, & Contreras-Vidal, 2017). Excitatory and inhibitory activity at the dendrites of large columns of neurons near the cortical surface causes changes in local electrical potential through the flow of charged

ions across the membrane. The human brain has an average of 10^4 neurons per mm^3 (Teplan, 2002) while the average scalp EEG electrode covers an area of approximately 1.6 cm^2 (Lopez-Gordo, Sanchez-Morillo, & Valle, 2014). Because of this mismatch in scale, as well as the signal distortion that come from passing through the tissues between the electrode and the cortex, the spatial resolution of the EEG is very poor.

Further complicating analysis of the EEG is the contamination of both subject-induced and environmental artefacts. The changes in voltage being recorded are in the microvolt range (Teplan, 2002), small enough to be obscured by powerline interference (60 Hz in America, 50 Hz in Europe and Asia). Subject motion or muscle activation from activities such as blinking or swallowing can also cause changes in the recorded voltages and distort EEG recordings.

1.3.2 Alpha Waves

The alpha rhythm, an 8-13 Hz oscillation in average voltage, is a commonly used for studies in brain dynamics as well as for signal quality evaluation because it is both easy to identify on sight and easily induced. When the eyes close there is a dramatic increase in the power of the alpha band, particularly in the visual cortex in the occipital region. This effect, known as the Berger effect (Kirschfeld, 2005), was theorized to be a resumption of an idling rhythm induced by the lack of input (Toscani, Marzi, Righi, Viggiano, & Baldassi, 2010). However, other studies suggest that the change in alpha is correlated with changes of attention to visual stimuli rather than input itself (Clayton, Yeung, & Cohen Kadosh, 2018).

CHAPTER 2. METHODS

2.1 Overview

The purpose of this study is to compare the abilities of different spatial filtering techniques to characterize and localize features of the EEG. 11 subjects were recruited to the study, which was approved by the IRB at the University of Kentucky. After obtaining informed consent, subjects were seated in front of a computer display and led through a sequence of repetitive actions that included repetitive eye closure and hand contraction. Specialized electrodes were used to simultaneously record referential and Laplacian scalp potentials at 12 locations on the scalp during this protocol. The data were analyzed using five different spatial filters to characterize the relative changes in alpha rhythm power and spatial coherence during the eye closure and motor tasks.

2.2 Data Collection

2.2.1 Subjects

A total of 11 healthy individuals (mean age 25.5 ± 4.7 years) were recruited from the student body at the University of Kentucky and the general population from 18-32 years of age, with no restrictions on dominant hand or ethnic/minority status.

2.2.2 Tripolar Concentric Ring Electrodes

This study makes use of a new kind of electrode called a tripolar concentric ring electrode (TCRE). The outer ring of the TCRE measures voltages the same as a conventional gold cup electrode which allows simultaneous recording of an EEG and calculating the Laplacian of the central disk. As no other distant electrodes are needed this

single electrode offers a more focal Laplacian estimate independent of any other recordings (Alzahrani, 2019). This focal Laplacian has been shown to offer improved spatial resolution over other methods of estimating the Laplacian (Liu, Makeyev, & Besio, 2020).

However, application of electrodes individually is a time-consuming process. Electrode placement must be precisely marked prior to scrubbing the scalp and attaching the electrodes with an adhesive, conductive paste. There is a limit on how long subjects can be expected to sit for studies in a laboratory setting and the more time that is required to set up the equipment the less time there is for actual data collection. It is therefore common practice in laboratory setting to embed electrodes into a cap that will hold all the electrodes in place simultaneously, requiring only a brief time spent measuring to align the cap and inject a conductive gel. To this end a set of electrode holders were developed for easier electrode placement and scalp preparation.

2.2.3 Tasks

Brief EEG recordings were made using a commercially available triconcentric ring electrode (TCRE) system (t-Interface 20, CREmedical, Kingston, RI, USA) and a biosignal amplifier (g.HIamp 256 biosignal amplifier, g.tec) from subjects who were instructed to engage in an alpha modulation task followed by a movement task. For the alpha modulation task subjects were instructed to alternate between opening and closing their eyes for 30 seconds five times in succession. This sequence was repeated twice for each subject yielding a total of 10 periods with the eyes closed and 10 with the eyes open for each subject.

Subjects were seated comfortably during the tasks in front of a computer monitor. Gold cup electrodes were attached using Ten20 conductive electrode gel to the right and left mastoids to serve as reference and ground, respectively. The impedance between the ground and reference electrodes was verified to be below 3 k Ω . Impedance values were measured using a checktrode (1089 mk III, UFI, California). The subject then put on the elastic cap with 3D-printed holders for the TCRES embedded in it at 12 scalp locations (F3, Fz, F4, C3, Cz, C4, P3, Pz, P4, PO7, POz, and PO8) according to the International 10-20 system of electrode placement. The cap was centered on the subject's scalp so that Cz was located midway between the nasion and inion and the right and left tragus. The scalp was then abraded to reduce skin impedance using a cotton swab and Nuprep gel. Using a plastic syringe, TD-246 conductive paste (Florida Research Instruments) was applied to each recording location on the scalp and surface of the corresponding TCRES to ensure good contact. Impedances between each TCRES and the reference electrode were measured using the checktrode and ranged from 6.0 to 24.4 k Ω with a median value of 10.5 k Ω over all recordings. The TCRES were connected to the t-interface, with a gain of \sim 187x, which was then connected to the g.tech biosignal amplifier through a g.HIamp headbox. Signals were passed through a 0.1-100 Hz Butterworth bandpass filter prior to sampling at 256 Hz.

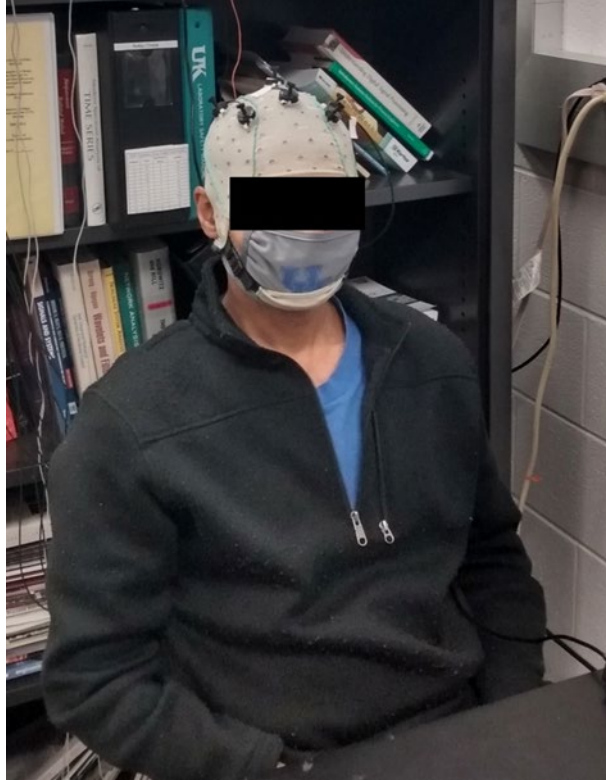


Figure 2.1 Subject seated with cap and electrodes on.



Figure 2.2 Close up of electrodes in the cap

2.3 Signal Analysis

2.3.1 Overview

The EEG is sensitive to artefacts and signal quality is critical to avoid coming to the wrong conclusion in any analysis. The reading at the reference electrode, placed at an electrically inactive location on the body such as the mastoid or earlobe, is removed from the sensing electrode placed at the location of interest at which neural activity is to be examined. Any electrical signal present in the earlobe can be safely assumed to not be related to activity in the brain.

Five different signals were derived for each TCRE lead: 1. The EEG potential (eEEG) measured from the outer ring of the TCRE (this is equivalent to conventional referential EEG); 2. A common average referenced signal (CAR) obtained by subtracting the mean over all twelve eEEG signals from the sensing electrode in the location of interest; 3. A local average reference (LAR) using the same method as the CAR but using the mean of each electrode and its nearest neighbors instead of all 12; 4. A local Laplacian potential (LL) estimated using finite difference approximations; and 5. A focal Laplacian (FL) estimated in hardware by combining the potentials measured at the three concentric rings of the TCRE (Besio, Koka, Aakula, & Dai, 2006).

2.3.2 Common Average Reference

Rather than use a single reference location, the average of all the electrodes is often used. This derivation, known as a common average reference, has the effect of removing common mode artefacts (Ludwig et al., 2009)– i.e., artefacts that contaminate all electrodes – and is particularly useful in noisy recordings where small variations are expected (Essl &

Rappelsberger, 1998). The voltage for the CAR derivation for a given electrode is calculated by subtracting the mean voltage of all the electrodes in the montage from the electrode being referenced.

$$V_{CAR} = V_k - \sum_{i=1}^n \frac{V_i}{n}$$

Figure 2.3 Formula for calculating the voltage for a given location using the CAR method. In this formula V_k is the voltage of the electrode for the location being considered and n is the total number of electrodes in the montage.

2.3.3 Local Average Reference

For the LAR derivation the method is similar to the CAR but with a subset of the electrodes. The mean of the sensing electrode's voltage and the voltages of 4 nearby electrodes is subtracted from the voltage of the sensing electrode. The 4 nearby electrodes were chosen in keeping with the electrodes used in the Laplacian derivation.

$$V_{LAR} = V_{F3} - \frac{V_{F3} + V_{Fz} + V_{F4} + V_{C3} + V_{P3}}{5}$$

Figure 2.4 LAR formula for the F3 electrode

2.3.4 Laplacian

The Laplacian calculates the divergence of the gradient of a function in space. For an EEG this means looking at the overall distribution of voltages to find the current being

injected at a particular location. This can be estimated in the EEG using the finite difference method.

The finite difference method for approximating the Laplacian is based on a Taylor series expansion of the spatial potential function and follows the approach developed in (Carvalhoes & de Barros, 2015). For a bivariate function, as is needed for a two dimensional grid of electrodes, partial derivatives are used for the expansion.

$$\begin{aligned}
V(a + h_1, b + h_2) &= V(a, b) + \left[\frac{\partial V(a, b)}{\partial x} h_1 + \frac{\partial V(a, b)}{\partial y} h_2 \right] \\
&+ \frac{1}{2} \left[\frac{\partial^2 V(a, b)}{\partial^2 x} h_1^2 + \frac{\partial^2 V(a, b)}{\partial x \partial y} h_1 h_2 + \frac{\partial^2 V(a, b)}{\partial^2 y} h_2^2 \right] \\
&+ \frac{1}{6} \left[\frac{\partial^3 V(a, b)}{\partial^3 x} h_1^3 + \frac{\partial^3 V(a, b)}{\partial^2 x \partial y} h_1^2 h_2 + \frac{\partial^3 V(a, b)}{\partial x \partial^2 y} h_1 h_2^2 + \frac{\partial^3 V(a, b)}{\partial^3 y} h_2^3 \right] \\
&+ \dots
\end{aligned}$$

Figure 2.5 The Taylor series expansion for calculating the Laplacian for a location on a 2 dimensional grid

h_1 and h_2 are incremental distances along x and y directions. Note that we have made the simplifying assumption of a two-dimensional grid of electrodes with no effect of curvature of the scalp. In the montage used, we have 3 conditions for which we will need to simplify the equation above: 1. *Center*: where the electrode has 4 electrodes surrounding it in the anteroposterior and lateral directions (a “plus” neighborhood); 2. *Edge*: where there are 3 immediate neighboring electrodes; and 3. *Corner*: where there are only two

immediate electrode neighbors. These approximations have been described and validated in the literature (Carvalhoes & de Barros, 2015).

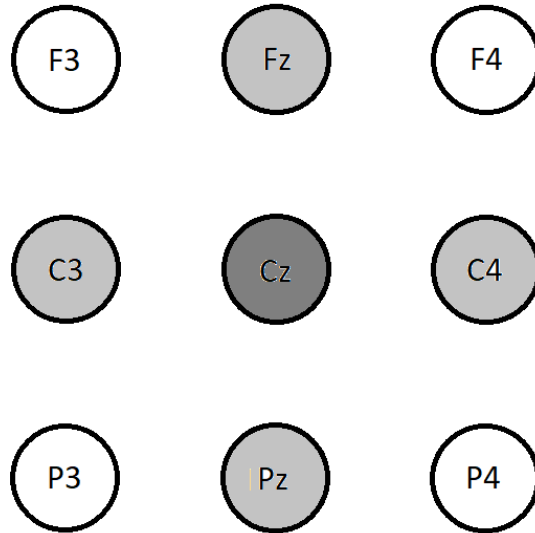


Figure 2.6 Example of a center electrode

$$\text{Lap}(V(a, b)) \approx \frac{V(a + h, b) + V(a - h, b) + V(a, b + h) + V(a, b - h) - 4V(a, b)}{h^2}$$

Figure 2.7 Simplified formula for the Laplacian of a center electrode

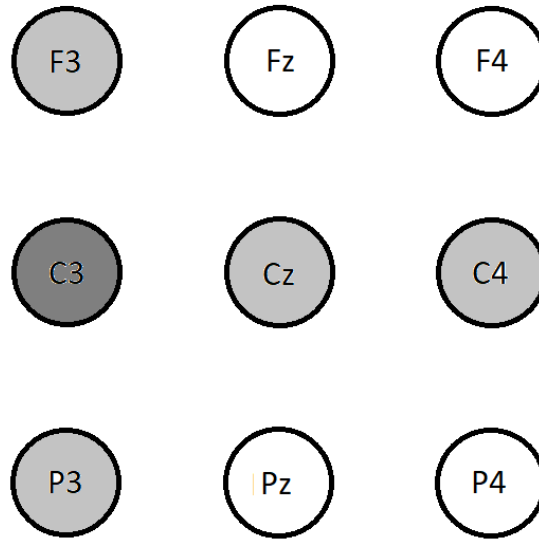


Figure 2.8 Example of an edge electrode

$$Lap(V(0, b)) \approx \frac{V(2h, b) - 2V(h, b) + V(0, b + h) + V(0, b - h) - V(0, b)}{h^2}$$

Figure 2.9 Simplified formula for the Laplacian for an edge electrode

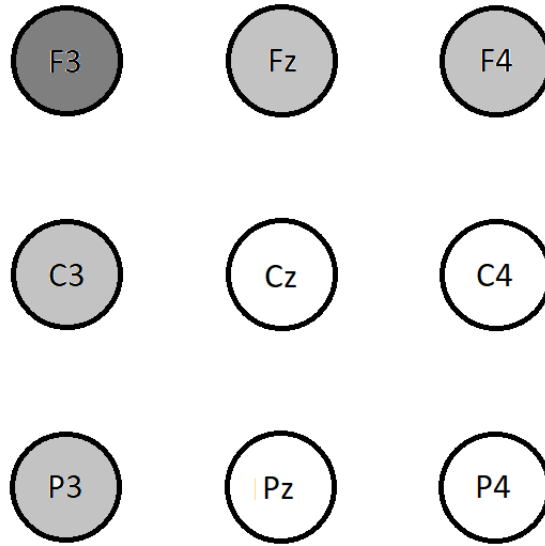


Figure 2.10 Example of a corner electrode

$$\text{Lap}(V(0, b)) \approx \frac{V(2h, b) - 2V(h, b) + V(0, b - 2h) - 2V(0, b - h) + 2V(0, b)}{h^2}$$

Figure 2.11 Simplified formula for the Laplacian of a corner electrode

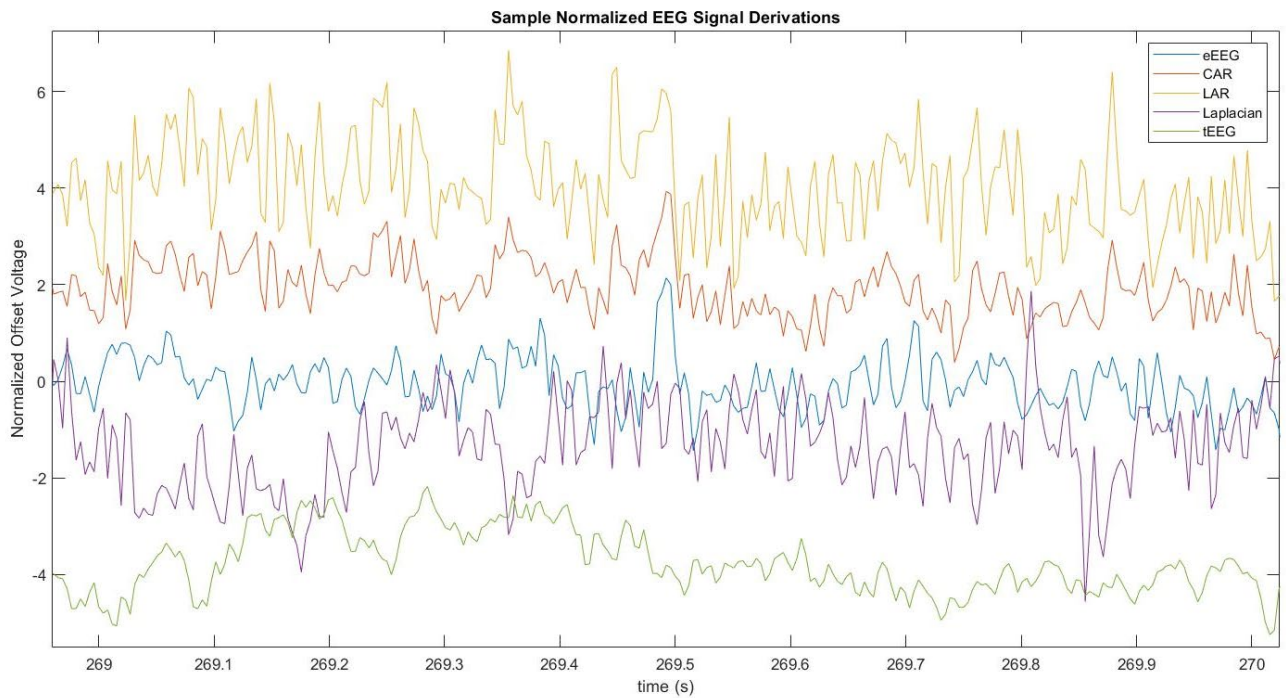


Figure 2.12- EEG signal derivations. All signals were normalized for visual comparison.

2.3.5 Electrode Holders

Custom electrode holders were designed using a ring and cylinder design. Holders were 3D-printed from thermoplastic polylactic acid (PLA) and thermoplastic polyurethane (TPU). The ring portion of the holders were inserted into an elastic cap at the desired 10-20 locations. This cap was then stretched over the subject's scalp and centered. The opening in the rings was large enough to access the scalp for cleaning with Nuprep and a cotton swab. TD-246 was also applied through this opening. Electrodes were inserted into the TPU cylinder and held firmly in place with a .5 mm thick lip. The cylinder was then inserted into the ring and twisted clockwise to lock the cylinder into the ring.

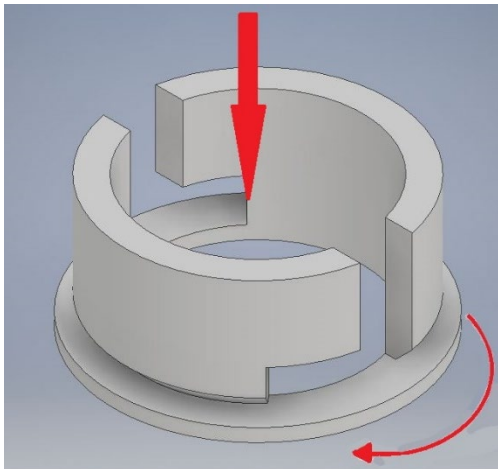
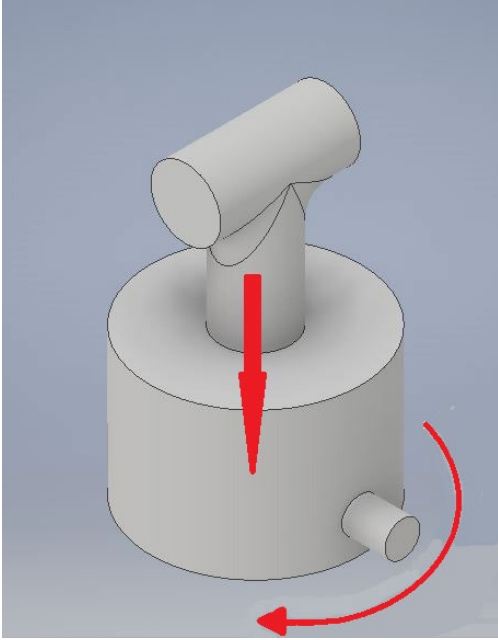


Figure 2.13 Electrode holder assembly. Red arrows indicate direction of motion for insertion.

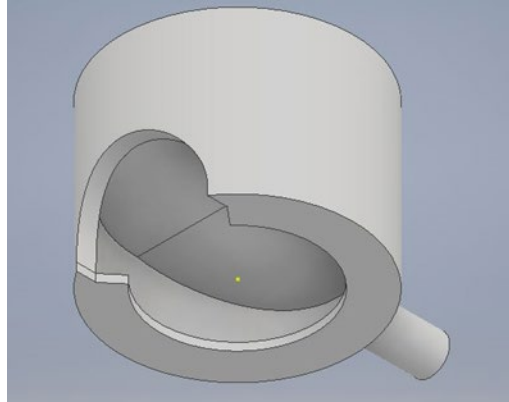


Figure 2.14 Electrode holder model seen from below. The thin lip around the edge is flexible enough to allow the electrode to be inserted. The holder is flexible and deforms slightly when the electrode is inserted, which allows the electrode to be held firmly in place

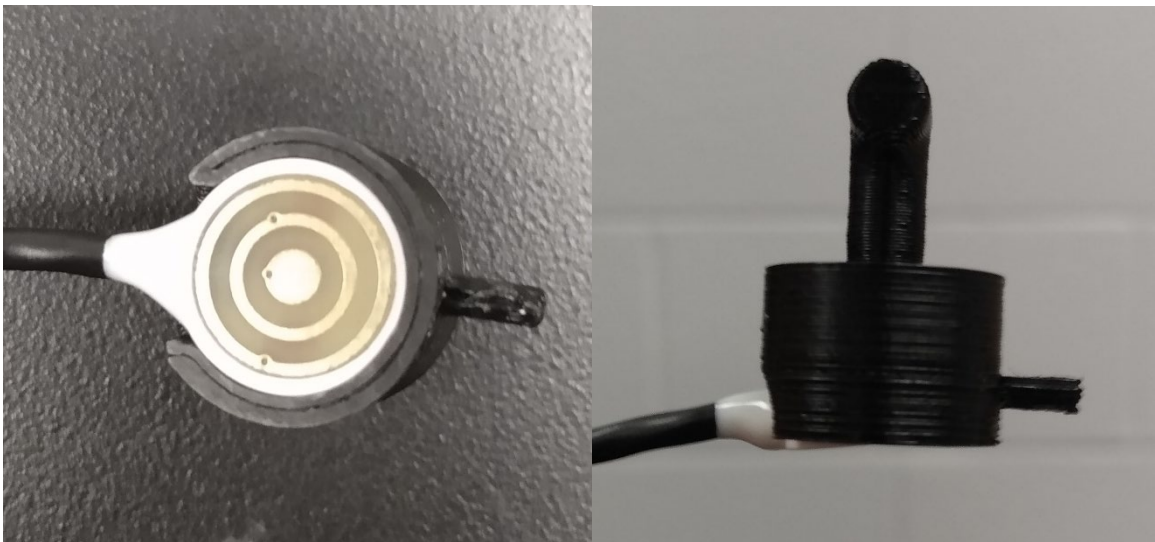


Figure 2.15 A TCRE in the holder

The higher impedance values are known to reduce the amplitude of an EEG signal reducing the signal to noise ratio (SNR). The generally accepted maximum value of impedance with TCRE's is $10\text{ k}\Omega$ (Besio et al., 2006; Besio & Prasad, 2006; Koka & Besio, 2007; Mathewson, Harrison, & Kizuk, 2017), slightly lower than the mean impedance value recorded in this experiment, though some say up to $20\text{ k}\Omega$ is acceptable (Lopez-Gordo et al., 2014). To evaluate the effect that higher impedance has on this recording

setup two comparisons were made. First, the percentage of the signal that was powerline noise was calculated taking the power of the powerline band (58-62 Hz) and dividing it by the total power of the signal. This percentage was then compared to the measured impedance using the Pearson correlation coefficient. This was repeated for the five signal derivations to be analyzed in this study. Second, as we are primarily looking at the alpha band in this study, we also looked for any differences in the percentage of the signal in the alpha band. The power of the alpha band over the entire recording was divided by the total power of the recorded signal after using a 4th order Butterworth band stop digital filter to remove the powerline noise. This alpha percentage was then also compared to impedance for all derivations using the Pearson correlation coefficient.

2.4 Amplitude of event-related alpha modulation in terms of signal power

Each of the four signals thus derived were then filtered into the alpha band (8-13 Hz) using a 4th order Butterworth digital filter applied in both directions to recover phase and the envelope of the Hilbert transform calculated. The magnitude of the Hilbert envelope, a measure of the instantaneous power of a signal (Benitez, Gaydecki, Zaidi, & Fitzpatrick, 2001; Johansson, 1999), was further lowpass-filtered down to 1 Hz to reduce noise fluctuation and then scaled by the mean value in the 3-second period immediately before eye closure. The average value of the scaled envelope in the 10-second period after eye closure was used as an estimate of alpha reactivity. The alpha reactivity produced by the five signal derivations were compared using repeated measures analysis of variance (rmANOVA) and post hoc analysis using Tukey's honest significant difference test (Tukey's HSD).

2.5 Spatial localization measured through signal coherence

Using the phase angle calculated with the Hilbert transform mean phase coherence (MPC), a measure of phase synchrony, was used to identify mutual interference between the signals generated in different regions.

$$MPC = \frac{1}{N} \sum_{i=1}^N |e^{j(\Phi_{i1} - \Phi_{i2})}|$$

Figure 2.16 Formula for the calculation of mean phase coherence. Φ is the instantaneous phase angle calculated by the Hilbert transform.

For each of the derived signals the MPC of each 30 second window of eye closure was calculated for each of the 66 possible unique electrode pairs using the Hilbert phase angle. The resulting sets of MPC were compared to the distance between the electrodes.

Distance between electrodes was calculated assuming a standardized distance based on the 10-20 method of electrode placement. The distance between neighboring electrodes, such as Pz and POz or Cz and C1, is assumed to be 1. The PO electrodes are far enough back on the scalp that this assumption no longer appears to be true so electrodes PO7 and PO8 were selected as the closest option to keep a rectangular montage.

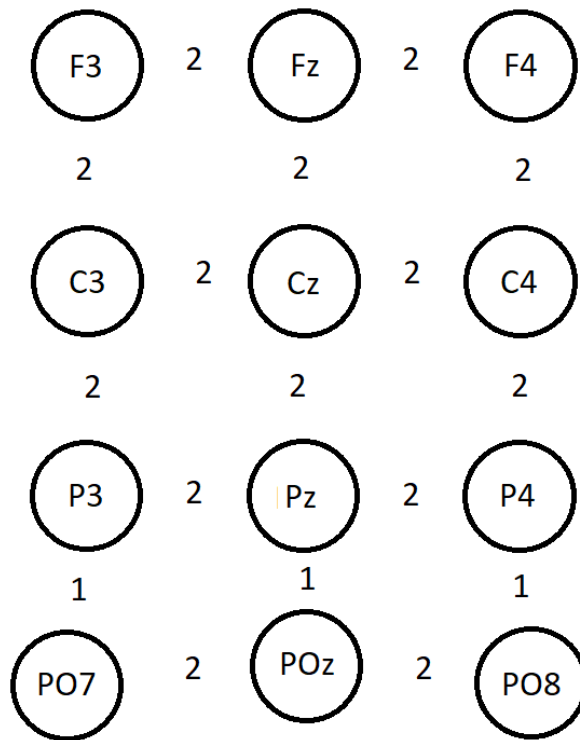


Figure 2.17 Proportional distances between electrodes in the montage. Most are two increments apart but the distance between P and PO is only 1. These electrodes were chosen to keep the montage as rectangular as possible for LL calculations.

To identify any response in MPC related to alpha modulation the MPC for each of the derived signals was again calculated but in a three second moving window advancing with a one quarter second increment. The mean MPC for the ten seconds post eye closure was divided by the mean MPC for the three seconds preceding eye closure and compared using an rmANOVA and Tukey's HSD.

CHAPTER 3. RESULTS

3.1 Effect of Impedance on Powerline Noise and Alpha Detection

The impedance at an electrode did not have a significant impact on the signal-to-noise ratio of the EEG recorded from it. The powerline noise, estimated here as the average percent of the signal power in the 58-62 Hz band, is shown to be more impacted by the signal derivation applied than by the impedance. None of the signal derivations show a meaningful correlation between line noise and electrode impedance ($r^2 < 0.035$). However, there was considerable variation in the powerline noise depending on which signal derivation was used. The FL shows lower mean powerline noise of 35.42%, less than half that of CAR which was the second lowest at 71.20%.

The percentage of the power in the alpha band was also shown to not be correlated with impedance. In this case the FL and CAR methods showed greater percentage of alpha in their signals, but no signal derivations showed any correlation between alpha and impedance ($r^2 < 0.057$).

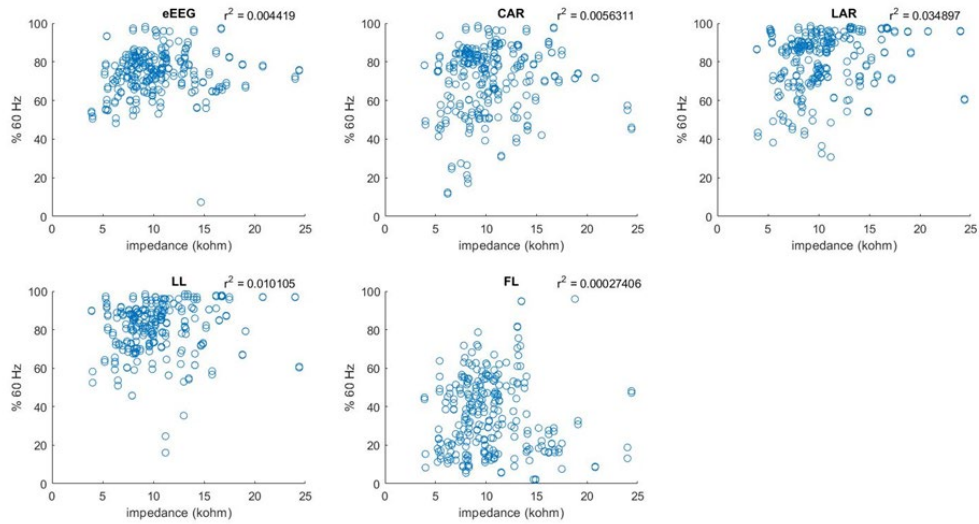


Figure 3.1 Relation between the powerline noise in the signal and impedance of the electrode for each derivation. Most of the signals have very high line noise, which does partially obscure the underlying signals without a notch filter, but notice this is not the case for the FL.

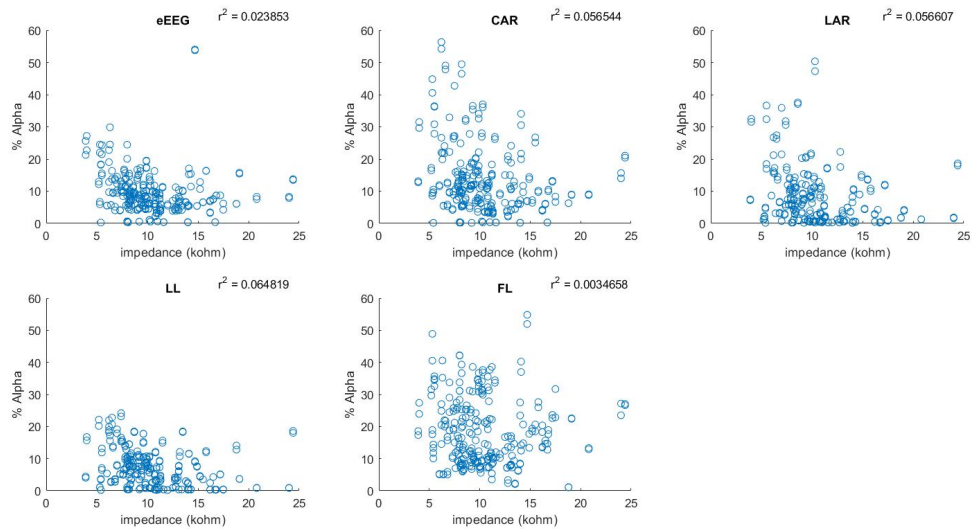


Figure 3.2 Relation between the alpha power in the signal and impedance of the electrode for each derivation. These percentages are after a notch filter has removed the powerline noise.

Table 1 Summary of statistics for the signal-impedance comparisons.

Derivation	Mean % powerline noise	r ²	Mean % alpha	r ²
eEEG	74.15	0.0044	9.25	0.024
CAR	71.20	0.0056	13.16	0.057
LAR	80.81	0.035	7.59	0.057
LL	79.15	0.0014	7.49	0.064
FL	35.42	0.00027	18.06	0.0035

3.2 3.2 Effect of Spatial Filtering on the Strength of Alpha Reactivity

Averaging the alpha reactivity of the derived signals across all subjects and channels shows significant ($p < .05$) differences. The CAR derivation showed significantly greater alpha reactivity than any other method while the eEEG, LAR, and FL were all significantly ($p < .05$) more reactive than the LL.

Comparing the differences in alpha reactivity between regions (Frontal, Central, Parietal, and Parietal-Occipital) reveals a general trend of increased alpha reactivity as the electrodes move from the anterior to the posterior of the of the scalp. This difference is most pronounced in the LL derivation with a clear difference between the anterior (F and C) versus posterior (P and PO). Further, the CAR derivation showed greater alpha reactivity in all regions compared to the other methods.

Comparing the mean differences between regions clarified the general trend of alpha reactivity increasing from anterior to posterior regions. The LL shows this gradient most clearly with each region showing significantly ($p < .05$) greater reactivity than the

preceding region. Both the FL and eEEG also show this trend though not perfectly; the C electrodes registered as slightly, though not significantly, lower in reactivity than the F electrodes in both derivations and the eEEG only shows significant difference between the anterior regions (F and C) and the posterior regions (P and PO). The CAR and LAR however did not follow this trend with the C region registering as the least reactive region.

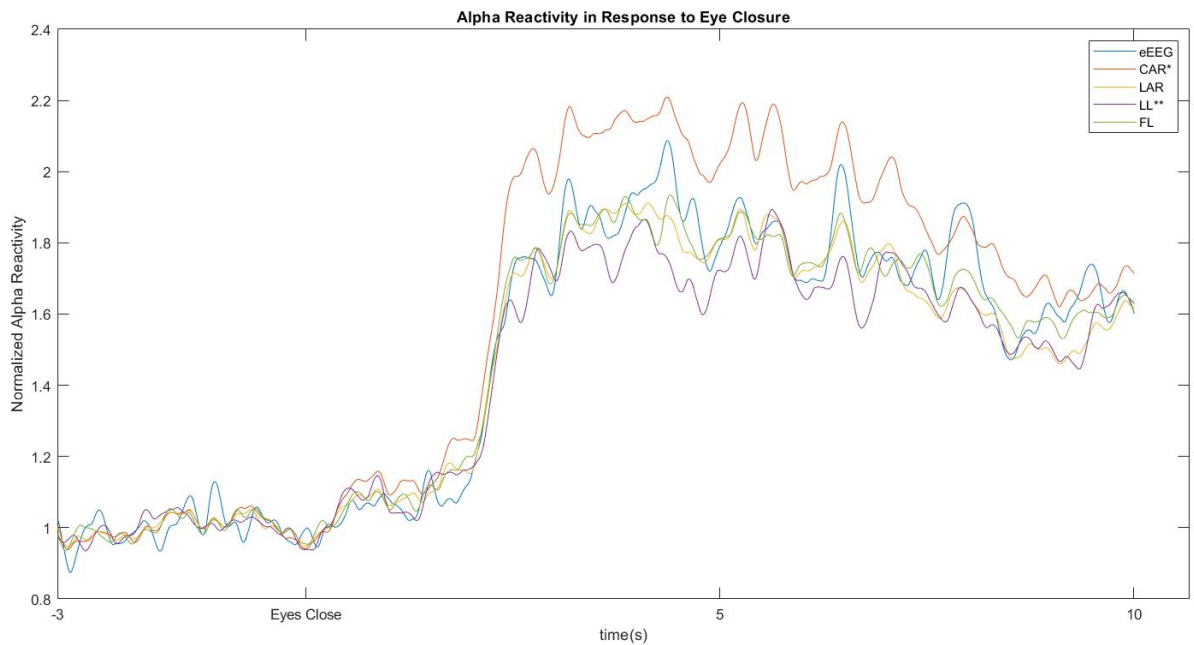


Figure 3.3 The average change in the magnitude of the Hilbert envelope of the alpha band in response to eye closure. Each signal is scaled by dividing the signal by the mean of the first 3 seconds.

*indicates significantly ($p < .05$) greater alpha reactivity than all other derivations.

** indicates significantly ($p < .05$) lower alpha reactivity than all other derivations

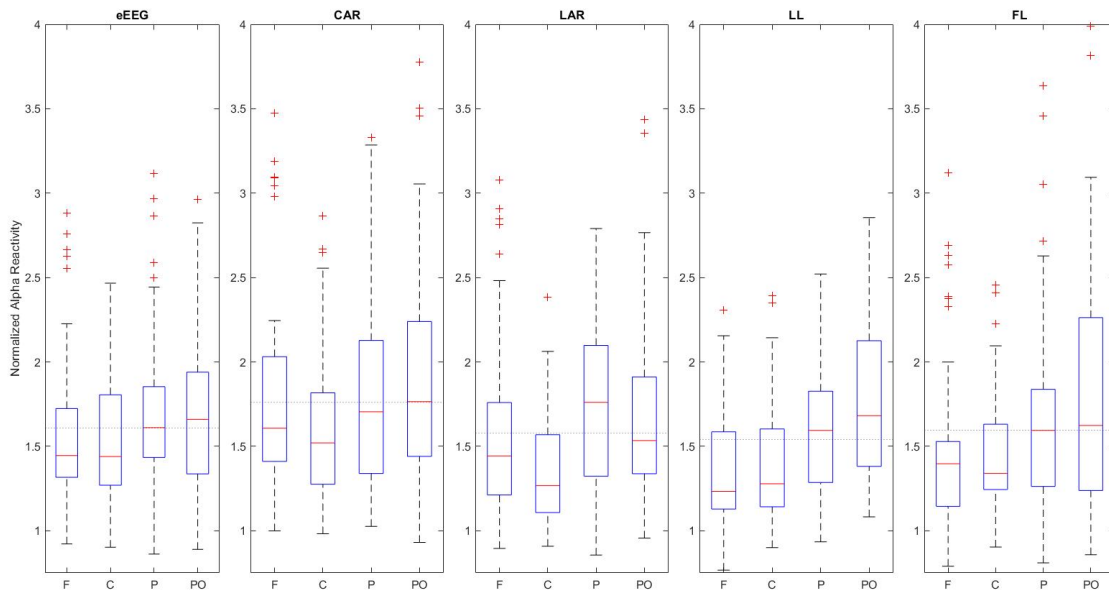


Figure 3.4 The distribution of the alpha reactivity of each region. The grey line indicates the overall mean alpha reactivity of the derivation.

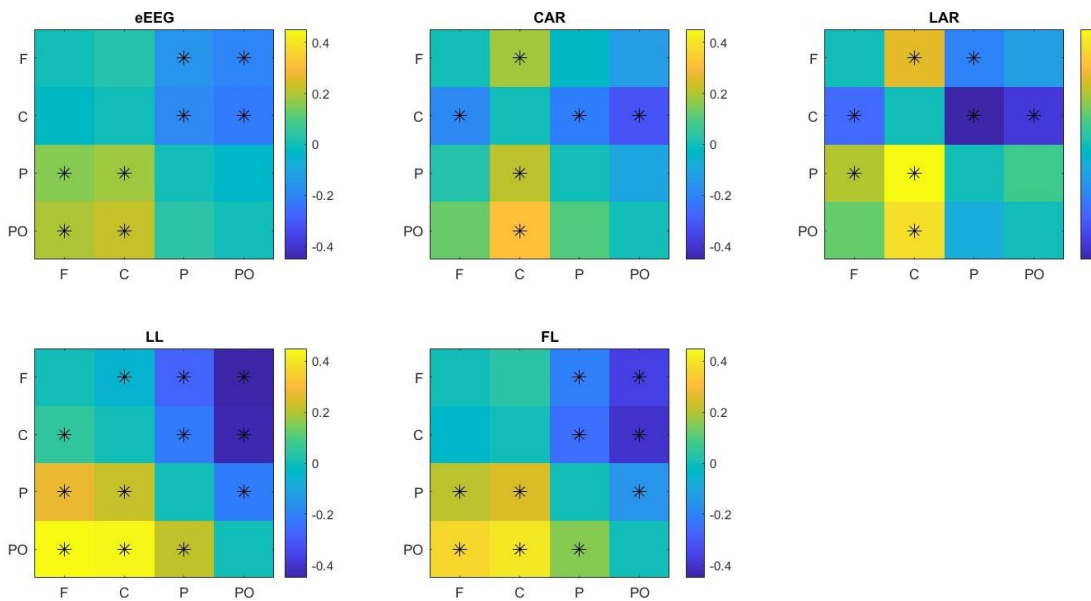


Figure 3.5 The mean difference between the alpha reactivity of compared regions. A * indicates significance with $p < 0.05$

3.3 Effect of Spatial Filtering on Alpha Band EEG Coherence Between Regions

MPC is greatly affected by spatial derivation. The eEEG is shown to have significantly higher MPC than any other derivation. Further, MPC can be seen to respond to eye closure. The eEEG was the only derivation to not have a change in MPC in response to eye closure. The CAR derivation had the largest change in MPC in response to eye closure in both absolute and relative terms.

Distance between electrodes is shown to influence MPC. The eEEG is shown to have a linearly decreasing MPC as distance between electrodes increases. In the CAR, LAR, and LL derivations there is no relation between MPC and distance. In the FL we see a sharp decrease in the MPC at first before the trend levels off.

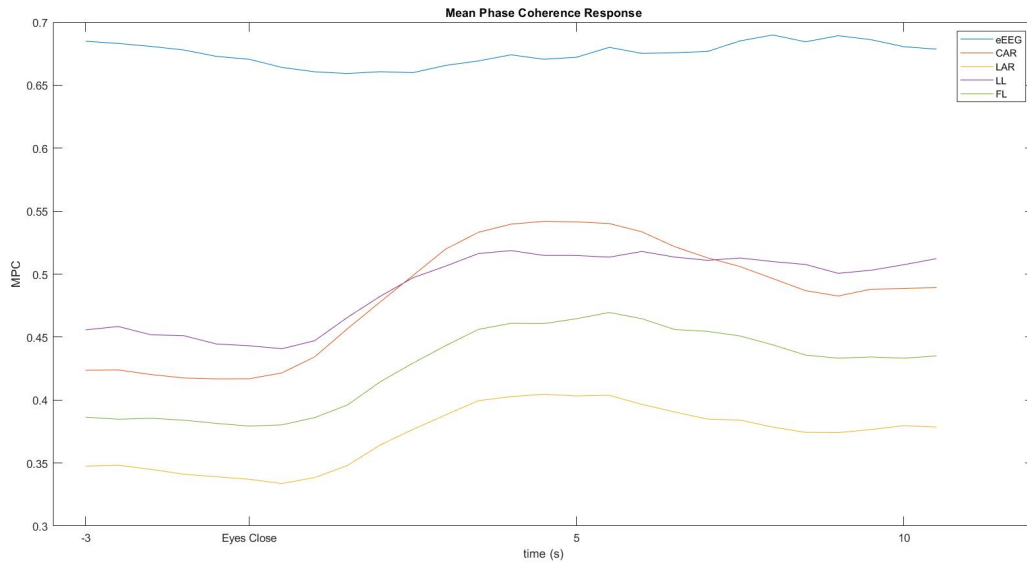


Figure 3.6 Mean phase coherence reactivity. The eEEG has the highest MPC and does not change significantly in response to eye closer. All other derivations show a significant ($p < .05$) increases in MPC when the eyes close.

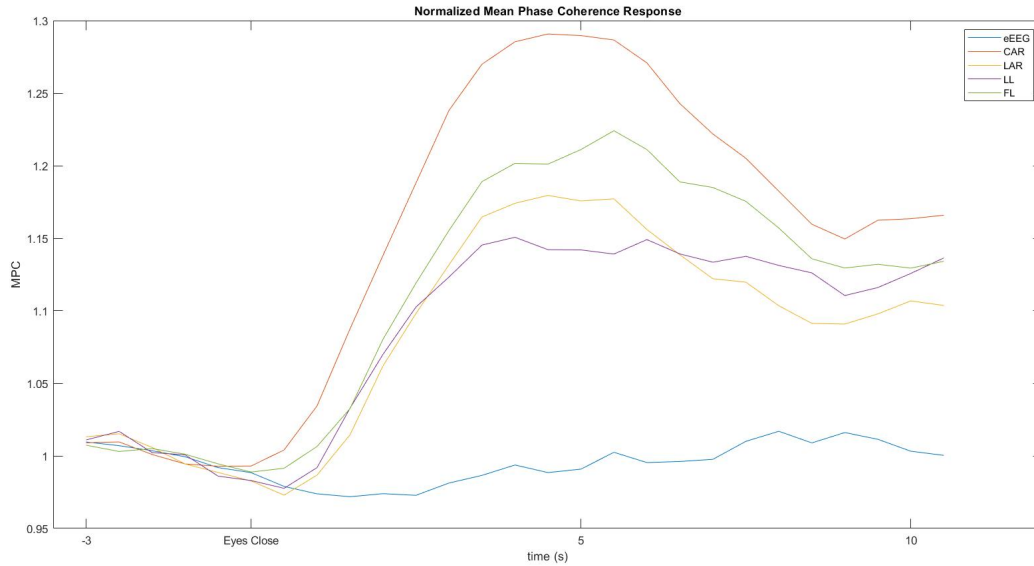


Figure 3.7 MPC responses divided by the mean of the first 3 seconds . This shows the CAR has a significantly ($p < .05$) greater response than any other derivation.

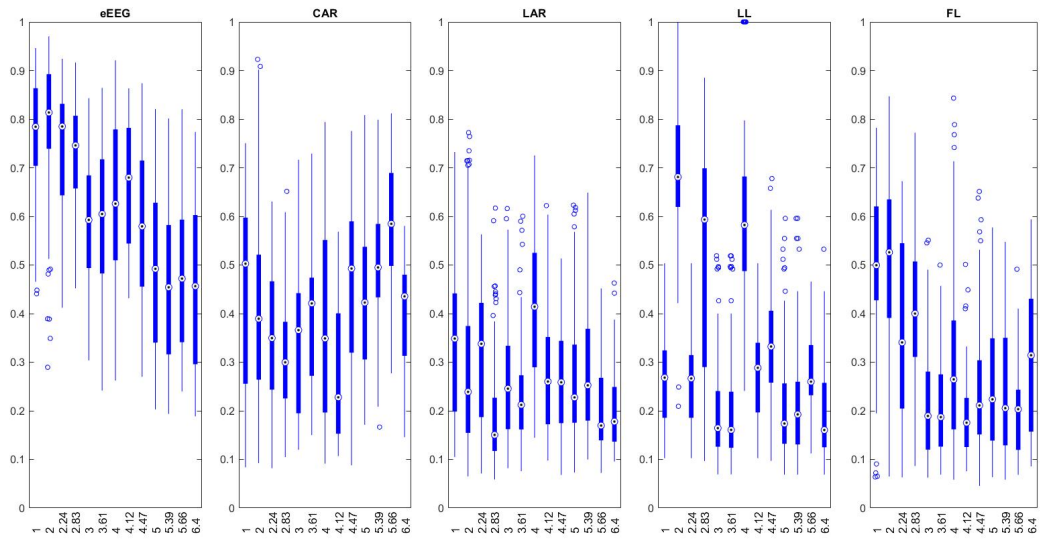


Figure 3.8 MPC vs Distance between electrodes for each of the signal derivations. The eEEG shows a relatively steady decrease in MPC as distance increases. There is a slight “stair step” like appearance to the values but that is not correlated with the difference between the distances observed. The FL shows a pronounced decrease in MPC over the first few comparisons before leveling out to a consistently low MPC.

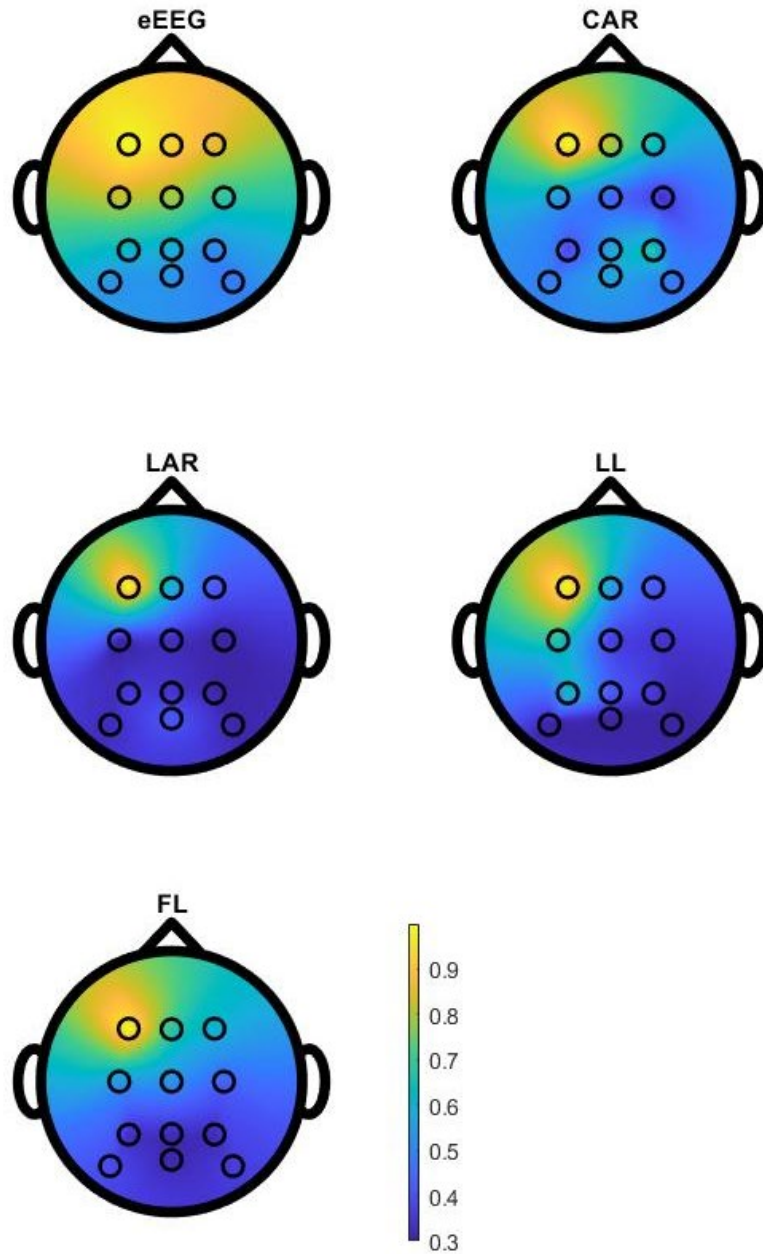


Figure 3.9 An illustrative example of the MPC compared to distance (Martínez-Cagigal, 2021). These results are for the F3 electrode but they are typical. The F3 electrode has an MPC of 1 in all cases because the signal is being compared to itself. Notice the CAR has a band of low MPC in the middle before it increases again. The eEEG has High over all MPC as well a steady decrease while the FL has a sharper decline.

CHAPTER 4. DISCUSSION

4.1 Overview

This work demonstrates the variability of signal characteristics depending on the signal derivation used. When considering signal localization the FL, through the use of TCREs, offers an improved ability to detect gradations in alpha reactivity and more focal signals as demonstrated by the rapid decay of MPC with increasing distance between electrodes.

4.2 Impedance vs Preparation Time

The variation in signal quality was not shown to be correlated with impedance in the ranges tested. Combined with improved set up times from the use of the cap the electrode cap as designed can be a useful tool to improve set up times without reducing signal quality. Further, the FL showed far less 60 Hz artefact than any other filtering method while the CAR method showed far more. This indicates that even with greater impedance values the use of TCREs can offer reduced signal noise compared to other filtering methods.

4.3 Alpha Reactivity to Eye closure

The simplicity of the CAR operation, in which you take the average of all available EEG signals and subtract that from each one, makes it an attractive choice for a spatial filter. However, it works on the assumption that common mode artefacts affect all channels similarly. By taking the average the individual variations are smoothed over and the common mode signal is emphasized and can be removed. However, if we assume the alpha

rhythm is mainly concentrated in the posterior regions of the cortex the CAR would induce a “false” alpha rhythm in the anterior regions by subtraction. This “false” alpha rhythm would be phase shifted by 180 degrees but would have more alpha power, and possibly reactivity, than it should. Therefore, the CAR should be used with caution and examined for possible skewing.

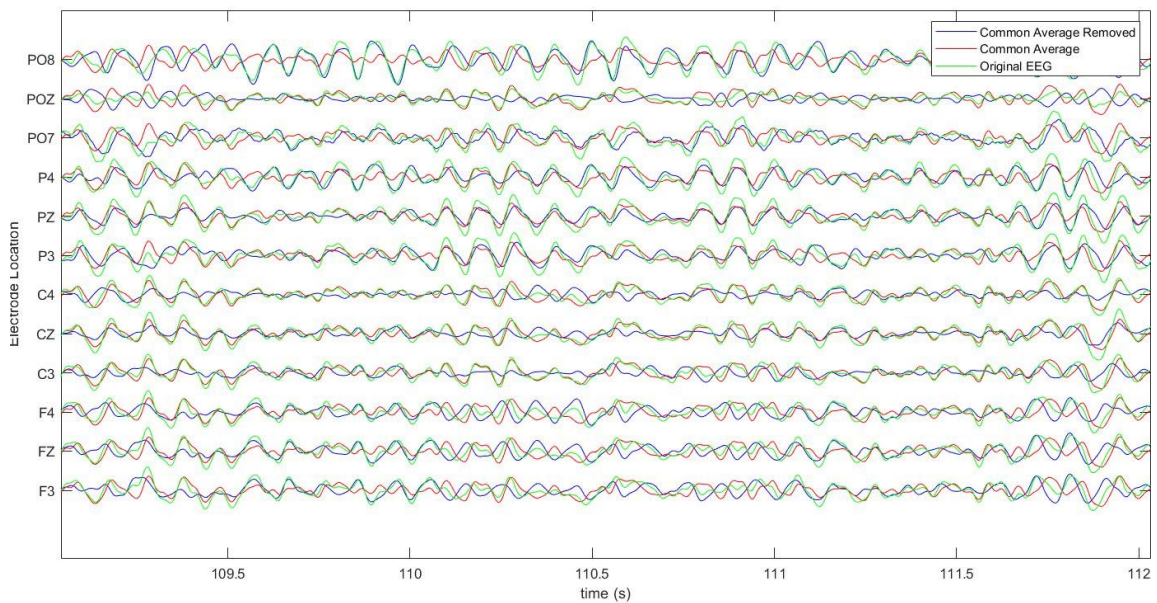


Figure 4.1 When the common average has significantly greater power in a particular bandwidth than a particular EEG signal subtracting the common average can cause an artificial increase in the power of that bandwidth. This set of signals shows some channels (F3, Fz, and F4 particularly between 110 s and 111 s) where the common average has a stronger alpha rhythm than the original EEG and has therefore induced a phase shifted alpha rhythm into it when it is subtracted out. Though not conclusive, this raises the possibility that the alpha reactivity in the CAR derivation is an artefact from high alpha reactivity in the posterior regions. More analysis is needed to conclude whether this artificial increase in alpha power is common enough and spatially focused enough to skew the results.

Though the LL had the lowest average alpha reactivity it had the highest spatial variation. In figure 15 the mean alpha reactivity progressively increases as we go from

anterior to posterior locations on the scalp, and so does the difference in the means. As alpha modulation is expected to be greatest in the posterior regions (Cantero, Atienza, & Salas, 2002) this gradient showed the LL derivation to have better spatial resolution in detecting alpha reactivity. The FL was nearly as selective as the LL only failing to identify a significant difference between the F and C regions.

4.4 Relation between MPC and Electrode Placement

Using MPC as a measure of spatial correlation in neural activity between locations on the cortex allows us to study signal localization by measuring changes in MPC as a function of the distance between the electrodes. If we assume that spatially distant locations are less likely to be connected (except through volume conduction) we expect MPC to decrease with distance. Therefore, the more rapidly the MPC decays with distance the better the spatial filter is deemed at localizing the signal.

This is shown clearly in the eEEG data, as the distance between electrodes increase there is a linear decrease in the MPC. In the FL however there is an exponential decrease showing that MPC drops quickly to a low value and then levels off once the electrodes are farther than adjacent in the montage used here (see figure 10). This suggests that the FL is better at filtering common mode artefact. The CAR, LAR, and LL all did not decrease in MPC with distance.

Phase coherence is often used to study coupling of cortical regions (Fein, Raz, Brown, & Merrin, 1988) and a method of quantifying the mutual information in two signals. It has been suggested that any conclusions about physiological responses, i.e.,

assuming communication between cortical regions, drawn from phase analysis should be done with caution (Fein et al., 1988; Rappelsberger, 1989; Schiff, 2005; Thatcher, 2010). However, as we are not looking to the phase as an indication of communication between regions but instead as a measure of interference caused by signals in distant regions of the brain this is not an issue.

4.5 Conclusion

Isolating epileptogenic zones in the cortex is necessary for the treatment of epilepsy that is not well controlled with medication. Improvements to signal localization in scalp EEG can reduce the area that needs to be examined with invasive intracranial EEG when identifying epileptogenic zones. The FL derived from the TCRE offers improved detection of signal dynamics and signal localization compared to a conventional EEG without the need for multiple electrodes.

4.6 Future directions

Further analysis of the CAR data is needed to identify how common and localized “false” alpha responses are. The motor task the subjects performed as part of this study will be analyzed using this methodology for identification of graded event related potentials in conjunction with other ongoing studies in our lab.

BIBLIOGRAPHY

- Alzahrani, S. I. (2019). *A comparison of tri-polar concentric ring electrodes to disc electrodes for decoding real and imaginary finger movements*. Colorado State University. Libraries,
- Bartolomei, F., Wendling, F., Vignal, J.-P., Kochen, S., Bellanger, J.-J., Badier, J.-M., . . . Chauvel, P. (1999). Seizures of temporal lobe epilepsy: identification of subtypes by coherence analysis using stereo-electro-encephalography. *Clinical Neurophysiology*, *110*(10), 1741-1754.
- Benitez, D., Gaydecki, P., Zaidi, A., & Fitzpatrick, A. (2001). The use of the Hilbert transform in ECG signal analysis. *Computers in biology and medicine*, *31*(5), 399-406.
- Besio, W., Koka, K., Aakula, R., & Dai, W. J. I. t. o. b. e. (2006). Tri-polar concentric ring electrode development for Laplacian electroencephalography. *53*(5), 926-933.
- Besio, W., & Prasad, A. (2006). *Analysis of skin-electrode impedance using concentric ring electrode*. Paper presented at the 2006 International Conference of the IEEE Engineering in Medicine and Biology Society.
- Bragin, A., Engel Jr, J., Wilson, C. L., Fried, I., & Mathern, G. W. (1999). Hippocampal and entorhinal cortex high-frequency oscillations (100–500 Hz) in human epileptic brain and in kainic acid-treated rats with chronic seizures. *Epilepsia*, *40*(2), 127-137.
- Cantero, J. L., Atienza, M., & Salas, R. M. (2002). Human alpha oscillations in wakefulness, drowsiness period, and REM sleep: different electroencephalographic phenomena within the alpha band. *Neurophysiologie Clinique/Clinical Neurophysiology*, *32*(1), 54-71.
- Carvalhoes, C., & de Barros, J. A. (2015). The surface Laplacian technique in EEG: Theory and methods. *International Journal of Psychophysiology*, *97*(3), 174-188.
- Clayton, M. S., Yeung, N., & Cohen Kadosh, R. (2018). The many characters of visual alpha oscillations. *European Journal of Neuroscience*, *48*(7), 2498-2508.
- Collinger, J. L., Foldes, S., Bruns, T. M., Wodlinger, B., Gaunt, R., & Weber, D. J. (2013). Neuroprosthetic technology for individuals with spinal cord injury. *The journal of spinal cord medicine*, *36*(4), 258-272. doi:10.1179/2045772313Y.0000000128
- Essl, M., & Rappelsberger, P. (1998). EEG coherence and reference signals: experimental results and mathematical explanations. *Medical and Biological Engineering and Computing*, *36*(4), 399-406.
- Fein, G., Raz, J., Brown, F. F., & Merrin, E. L. (1988). Common reference coherence data are confounded by power and phase effects. *Electroencephalography and clinical Neurophysiology*, *69*(6), 581-584.
- Guger, C., Spataro, R., Allison, B. Z., Heilinger, A., Ortner, R., Cho, W., & La Bella, V. (2017). Complete Locked-in and Locked-in Patients: Command Following Assessment and Communication with Vibro-Tactile P300 and Motor Imagery Brain-Computer Interface Tools. *Front Neurosci*, *11*, 251. doi:10.3389/fnins.2017.00251
- Johansson, M. (1999). The hilbert transform. *Mathematics Master's Thesis*. Växjö University, Suecia. Disponible en internet: http://w3.msi.vxu.se/exarb/mj_ex.pdf, consultado el, 19.

- Kirschfeld, K. (2005). The physical basis of alpha waves in the electroencephalogram and the origin of the “Berger effect”. *Biological cybernetics*, 92(3), 177-185.
- Koka, K., & Besio, W. G. (2007). Improvement of spatial selectivity and decrease of mutual information of tri-polar concentric ring electrodes. *Journal of neuroscience methods*, 165(2), 216-222.
- Li, G., Wang, S., & Duan, Y. Y. (2017). Towards gel-free electrodes: A systematic study of electrode-skin impedance. *Sensors and Actuators B: Chemical*, 241, 1244-1255.
- Liu, X., Makeyev, O., & Besio, W. (2020). Improved Spatial Resolution of Electroencephalogram Using Tripolar Concentric Ring Electrode Sensors. *Journal of Sensors*, 2020.
- Lopez-Gordo, M. A., Sanchez-Morillo, D., & Valle, F. P. (2014). Dry EEG electrodes. *Sensors*, 14(7), 12847-12870.
- Ludwig, K. A., Miriani, R. M., Langhals, N. B., Joseph, M. D., Anderson, D. J., & Kipke, D. R. (2009). Using a common average reference to improve cortical neuron recordings from microelectrode arrays. *Journal of neurophysiology*, 101(3), 1679-1689.
- Luu, T. P., Nakagome, S., He, Y., & Contreras-Vidal, J. L. (2017). Real-time EEG-based brain-computer interface to a virtual avatar enhances cortical involvement in human treadmill walking. *Scientific Reports*, 7(1), 1-12.
- Martínez-Cagigal, V. (2021). Topographic EEG/MEG plot. MATLAB Central File Exchange. Retrieved from <https://www.mathworks.com/matlabcentral/fileexchange/72729-topographic-eeg-meg-plot>
- Mathewson, K. E., Harrison, T. J., & Kizuk, S. A. (2017). High and dry? Comparing active dry EEG electrodes to active and passive wet electrodes. *Psychophysiology*, 54(1), 74-82.
- Mormann, F., Lehnertz, K., David, P., & Elger, C. E. (2000). Mean phase coherence as a measure for phase synchronization and its application to the EEG of epilepsy patients. *Physica D: Nonlinear Phenomena*, 144(3-4), 358-369.
- Rappelsberger, P. (1989). The reference problem and mapping of coherence: a simulation study. *Brain topography*, 2(1), 63-72.
- Schevon, C. A., Cappell, J., Emerson, R., Isler, J., Grieve, P., Goodman, R., . . . Kuzniecky, R. (2007). Cortical abnormalities in epilepsy revealed by local EEG synchrony. *Neuroimage*, 35(1), 140-148.
- Schiff, S. J. (2005). Dangerous phase. *Neuroinformatics*, 3(4), 315.
- Teplan, M. (2002). Fundamentals of EEG measurement. *Measurement science review*, 2(2), 1-11.
- Thatcher, R. W. (2010). Validity and reliability of quantitative electroencephalography. *Journal of Neurotherapy*, 14(2), 122-152.
- Toscani, M., Marzi, T., Righi, S., Viggiano, M. P., & Baldassi, S. (2010). Alpha waves: a neural signature of visual suppression. *Experimental brain research*, 207(3), 213-219.

VITA

Stephen Roy Dundon

Education:

Bachelor of Arts, May 2010

Hanover College, Hanover, Indiana

Bachelor of Science, May 2018

University of Kentucky, Lexington, Kentucky

Professional Positions:

Research Assistant, Neural Systems Lab

Department of Biomedical Engineering, University of Kentucky, Lexington, Kentucky